Characterization process to measure the electrical contact resistance of Gas Diffusion Layers under mechanical static compressive loads

Soufiane El Oualid, Rémy Lachat, Denis Candusso, Yann Meyer

AEM2016
Soufiane El Oualid; Oral-HE-Room-A-final
Abstract ID 224 - International Journal of Hydrogen Energy

Characterization process to measure the electrical contact resistance of Gas Diffusion Layers under mechanical static compressive loads

S. El Oualid [1, 2, 3], R. Lachat [2, 4], D. Candusso [3, 5], Y. Meyer [1, 2, ††, *]

[1] Univ. Bourgogne Franche-Comté, UTBM, Belfort, France
[2] FCellSys, Univ. Bourgogne Franche-Comté, UTBM, Belfort, France
[3] FCLAB (FR CNRS 3539), UTBM bâtiment F, Rue Thierry Mieg, F 90010 Belfort Cedex, France
[4] ICB UMR 6303, CNRS Univ. Bourgogne Franche-Comté, UTBM, Belfort, France
[5] IFSTTAR / COSYS / SATIE (UMR CNRS 8029), 25 Allée des marronniers, F 78000 Versailles Satory, France

* Corresponding author:
yann.meyer@utbm.fr

Tel: 0033 3 84 58 36 33
Fax: 0033 3 84 58 36 36

Other email addresses:
soufiane.eloualid@utbm.fr
remy.lachat@utbm.fr
denis.candusso@ifsttar.fr

International Journal of Hydrogen Energy
Volume 42, Issue 37, 14 September 2017, Pages 23920-23931

†† Research Associate at Sorbonne Universités, Université de Technologie de Compiègne, CNRS, UMR 7337 Roberval, Centre de recherche Royallieu, CS 60 319 Compiègne cedex, France

Abstract

Recent research has identified the mechanical properties of the fuel cell internal components (in particular, the Gas Diffusion Layers - GDLs) as key-parameters to obtain high final performances of the generator. The mechanical compression modulus of these components, the stability of their mechanical properties with respect to temperature and humidity, and their ability to interact with water have an impact on the electrical contact resistances in the stack and, by consequence, on the overall performance of the electric generator. Reducing the losses by contact resistance is an objective necessary to optimize the fuel cells in operation. The study of GDL electrical behavior under various internal operating conditions provides a suitable database to better understand their effects on the overall stack performance.
This paper describes an experimental method for measuring the electrical contact resistance versus the static mechanical pressure applied to the GDLs. A nonlinear behavior of the electrical contact resistance versus the mechanical stress is observed. The PTFE and MPL additions modify the electrical contact resistance.

Keywords:
Proton Exchange Membrane Fuel Cell; Gas Diffusion Layer; Mechanical properties; Compressive loads; Electrical contact resistances

Highlights:
• Three industrial GDLs are tested under static electromechanical excitations.
• A specific ex-situ electrical characterization method is developed.
• The electrical contact resistance is nonlinear versus the mechanical pressure.
• The electrical contact resistance decreases versus pressure at room temperature.
• The PTFE and MPL additions to the GDLs modify the electrical contact resistance.

1. Introduction

Fuel cell (FC) is one of the most promising solutions to generate power with high efficiency, portability and near zero-emissions [1, 2]. Proton Exchange Membrane Fuel Cell (PEMFC) or Polymer Electrolyte Fuel Cell (PEFC) is the most mature and promising FC technology due to the solid nature of its electrolyte, low start-up temperature and high efficiency. The PEMFC performance is fully related with the properties of its components, especially with the MEAs (Membrane Electrode Assemblies), with the assembly process to build a stack, and the operating conditions. The widespread success of this technology in the industry field is linked with the high performance provided by the stacks and the stable mechanical behaviors of the assemblies under both operating and environmental excitations. To reach suitable PEMFC performance levels and durability targets, it is essential to study both the electrical, thermal and mechanical behaviors of each MEA element under temperature and humidity variations [3]. Indeed, the coupling between the different physical phenomena inside the MEA leads to complex effects and interactions on the performance results. In particular, the compressive strength of the elements, the stability of their mechanical properties versus temperature, humidity, as well as their capabilities to interact with water have some direct effects on the electrical contact resistances inside the FC assembly, and thus, on the global performance of the whole generator. The decrease of the contact resistance losses is obviously required to optimize the global behavior of the PEMFC technology [4-12].
Gas Diffusion Layer (GDL) is known as a key-component of the MEA [13], due to its role in the gas diffusion and in the water flushing / management, high thermal and electrical conductivity, hydrophobicity, and mechanicals properties. Thus, understanding the compressive behavior of the GDL is required for further improvements of the PEMFC technology.

In the next part, we will present the different components of a PEMFC in terms of material and properties, allowing us to expose the operation mode of this generator in details and to highlight the strong mechanical / electrical interactions existing at the GDL / bipolar plate interfaces. The conclusions of Section 2 will underline the essentials points that have motivated us to realize this study focusing on the determination of the electrical contact resistances between gas flow field plates and Gas Diffusion Layers subjected to mechanical static compressive loads.
With this article, we intend to propose a better understanding of the GDL mechanical behavior as well as some guidelines for the ex-situ measurement of GDL electrical contact resistances. The work presented in this article is a step towards the more complex analysis of the mechanical – electrical GDL properties under real FC operating conditions including thermal and humidity variations.

2. The key-role of the GDL / bipolar plate interface

2.1. The FC assembly and its components

A PEMFC has four main components: the polymer electrolyte or membrane, the electro-Catalyst Layers (CLs), the Gas Diffusion Layers (GDLs), and the Flow Field Plates (FFPs) (or bipolar plates, gas distribution plates). Fig. 1 shows the classical architecture of a PEMFC. The Membrane Electrode Assembly (MEA) is built in an additive manner. The membrane is coated with Catalytic Layers (CLs) and assembled between two GDLs. In order to collect the electrons, the MEA and the GDLs are inserted between two bipolar plates. The reactants reach the cathode and anode sides through the channels of the FFPs and the GDLs. This minimal assembly is called cell. Each cell component is designed to realize specific functions in the MEA.

To generate a useful electric power, several cells are stacked and mechanically constrained by applying a clamping pressure from the terminal plates, usually with fasteners (bolts and nuts) [3, 14, 15]. As described by Jason Millichamp et al. in [10], various techniques used to put stacks into compression can now be found in the literature and be obtained from FC stack suppliers: standard tie rod setup, tie rods through gas / water manifolds, bands, crimps, straps / curved endplate, leaf-spring, tie rod springs, dynamic fluid compression plate.

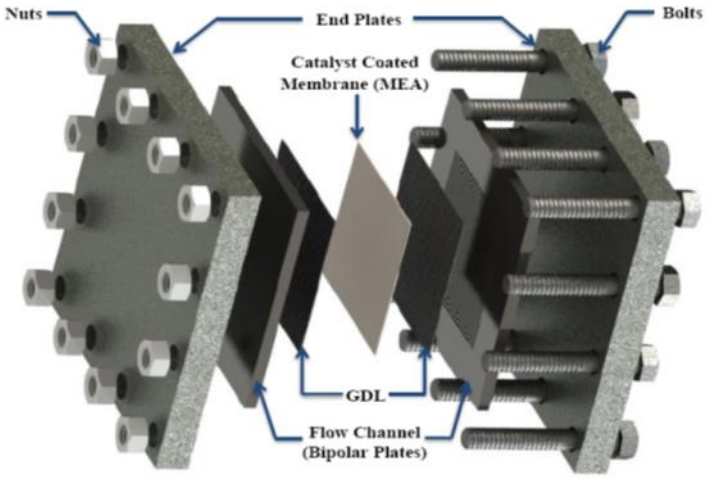

Fig. 1. Classical architecture of a PEMFC [16].

Polymer Electrolyte Membrane

PEM, also called a Proton Exchange Membrane, is an organic material providing the proton selectivity and forcing the electrons generated by Reaction (1) to travel along an external electric circuit to the cathode side; this is the key of the FC technology. Other substances passing through the electrolyte would tend to disrupt the chemical reaction.

Catalyst layers

A catalyst layer is added on both sides of the membrane at the anode and cathode sides, and lead to the MEA. Conventional PEMFC catalytic layers include particles of platinum dispersed on a high-surface-area of carbon support. This supported platinum catalyst is mixed with an ion-conducting polymer sandwiched between the membrane and the GDLs. The FC powers are generated by oxidizing hydrogen atoms into protons and electrons at the anode electrode (Reaction (1)), and by reducing oxygen atoms with protons at the opposite side (Reaction (2)).

$$H_2 \quad \leftrightarrow \quad 2\,H^+ + 2e^- \qquad (1)$$

$$\frac{1}{2}O_2 + 2H^+ + 2e^- \quad \leftrightarrow \quad H_2O \qquad (2)$$

Gas Diffusion Layers

The MEA is sandwiched between two GDLs. These elements provide the flow of reactants to catalytic sites, as well as the removal of product water. Each GDL is typically composed of a sheet of carbon paper in which the carbon fibers are partially coated with polytetrafluoroethylene – PTFE (note that metal-sheet GDLs also exist [14]). Gases rapidly diffuse through the pores of the GDL. These pores are kept open by the hydrophobic PTFE, which prevents excessive water buildup. In many cases, the GDL is coated with a thin layer of high-surface-area carbon mixed with PTFE, called the micro-porous layer (MPL). The MPL gives the possibility to manage retention of water to ensure electrolyte conductivity and gas flow inside the GDL.

The prediction of the GDL behavior is still challenging because of the complex geometries involved in the component. Numerous researches focus on the modelling of the GDL microstructure and on the parameters that affect its transport properties and performances (fiber diameter, GDL thickness, porosity, effect of PTFE loading, impact of clamping pressure) [13, 17-19].
Some mechanical degradation (compression, freezing-thawing, and erosion) and physicochemical degradation phenomena (chemical dissolution in solutions, electrochemical dissolution) affect the GDLs in the operating PEMFC [20]. From a mechanical point of view, GDLs are the FC components, which are the most prone to global or localized deformation since they exhibit the highest porosity (up to 80%). Beyond the issue of degradation, the compression of GDL has three main effects: change of the gas permeability and diffusion resistance, variation of the thermal and electrical contacts inside the GDL structure, impact on the electrical contact between the GDLs and the bipolar plates [20]. More details on these effects will be given in Section 3.

Bipolar plates
Commercial cells are built from a stack of MEAs in series with bipolar plates. These plates, which may be made of metal, carbon, or composites, provide electrical conduction between cells, as well as mechanical strength to the stack. The surfaces of the plates typically contain a "flow field," which is a set of channels machined or stamped in the plates in order to allow the gases to flow over the MEA (bipolar plates in stainless steel foam or metal foam are more rarely used [11]). We can also find some additional channels of liquid coolant inside the plates; these channels are used to manage the heat produced by the exothermic reaction between hydrogen and oxygen, and to achieve a higher performance and durability of the MEA elements [21, 22].
The bipolar plates are prone to different sources of degradation: mainly corrosion for the metal plates, mechanical stress and shocks. Some localized damages can also be induced by the bipolar plates inside the GDL structures, especially under the ribs of their flow patterns, quite less under the channels. Additional details will be provided on this issue in Section 3. As shown by R. Taspinar et al. through the development of a two-dimensional model that integrates a realistic bipolar plate and GDL interfacial morphology, this interface has also some effects on the mass, charge, heat transport and performance of PEMFCs. In particular, the simulations indicate that the Ohmic and concentration losses are increased [23].

2.2. Motivation for this work

An increase of the FC performance is notably the result of the progress realized on the design and architecture of components. The continuity of this progress is currently related to the deeper understanding of the physical phenomena occurring inside the stack.
The mechanical approach that we propose is original because it allows to study the mechanical behavior of the stack components linked with internal physics interactions in operating conditions or resulting from the stack assembly process.
When GDL properties are highly affected by compression, this study aims to propose an experimental approach to understand the effect of compression both on the GDL properties and PEMFC performance.

The following objectives were identified for the study:

- To develop a test bench of the ex-situ characteristics for a wide range of commercial GDLs.
- To develop a better understanding of the relationship between mechanical behavior and electrical contact resistances between GDL and bipolar plates.

- To identify the effect of GDL composition on the mechanical and electrical test responses.
- To study the effect of compression on the GDL properties and its influence on the global PEMFC performance.

In the following part, we will present the various methods to investigate the GDL physical properties related with the fibres structure. Also, we will discuss the effect of mechanical compression on the stack performances.

3. Ex-situ and in-situ investigation of GDL behavior

3.1. Structure investigations

GDL material structure provides useful functionality to this component:

- High thermal and electric conductivity
- Mechanical support to the MEA
- Management of the water flow, of the heat from the reaction
- Gas diffusion up to the catalytic layers.

The GDL structure is made of a structured carbon fibers layer. Two major structures are found in the different applications: woven (carbon cloth) and non-woven (carbon paper). The spatial location of the fibres has a direct effect on the mechanical properties of the GDL, as well as on the porosity, the permeability, and the electrical behavior [13, 24].

Porosity and pore size distribution

Porosity is the most important properties of GDL and all other physical properties (thermal conductivity, gas flow, mechanical behavior, water management) may be affected by its change. A porous material is also characterized by its porosity, denoted Ø and expressed by Eq. (3):

$$\emptyset = \frac{V_{p,t}}{V_{p,t}+V_s} \qquad (3)$$

With $V_{p,t}$ and V_s the pore volume (the volume of void-space) and the bulk volume respectively (mm^3). Porous materials have also cavities or channels which exist in a grain also called intra-granular pore: the pores can be open, closed or in intercommunication.

The porosity can be measured by a large set of techniques like gas absorption, mercury porosimetry, SEM or TEM [25, 26]. Mercury standard porosimetry (MSP) is the commonly used method. In the MSP technique, octane is used as an intrusion liquid to wet the GDL materials. This technique has the advantage of having very low injection pressures and providing a nondestructive investigation on any type of porous materials. The assessment of the pore size distribution is also a characterization method of porous materials. Due to the randomness in the structure of the GDL, the pore size is not uniform. MSP or MIP (Mercury Intrusion Porosimetry) can be used to measure this distribution [25, 26]. Yu-Xian Hang et al. [27] have studied the effect of the porosity gradient on the PEMFC performance, the water condensation on the open pores of the GDL, and the oxygen transport delay affecting the current density.

Surface roughness, fibre structure (SEM)

The GDL structure can be conditioned and modified to enhance its intrinsic properties. One of these modifications is to coat the carbon fibres surfaces with polytetrauoroethylene (PTFE). According to many studies, this solution has a significant effect under the operating conditions

on the mechanical behavior [28-31]. It ensures hydrophobicity of the GDL and protects the electrodes from flooding [30, 31].

Roughness of the substrate is another structural parameter of the GDL. Fishman et al. [32] have studied the effect of the surface topography. They have found that non-treated GDL surfaces with lower roughness have a high retention and a low evaporation of water [6, 33]. In order to create a smoother surface in contact with the CL, MPL provides a solution to eliminate the products of the chemical reaction and to increase the durability of the MEA.
During the PEMFC operation, the cell undergoes some changes in its dimension. This results in a mechanical stress inside the stack. This mechanical stress causes a modification of the mechanical behavior, of the electrical properties, and of the fluidic properties of the GDLs. This mechanical stress due to the operating conditions is added to the existing mechanical stress due to the assembly.

3.2. Effect of compression on stack performance (component properties)

The GDLs are designed to be able to withstand the internal mechanical pressure in the FC stack and ensure their main functionalities (gas flow, electrical conductivity, water management). To provide cell sealing (to avoid any gas leaks), mechanical clamping pressure is applied, as well as to minimize the contact resistance between the different components. The mechanical properties of a GDL are often evaluated with respect to the compressive elastic and plastic deformation, (ii) contact resistance, and (iii) the reactant flow under compression.

As already mentioned, the GDL is a composite structure with a high porosity rate, made by carbon fibers with the potential addition of a PTFE coating and the presence of a MPL. This leads to an elastic-plastic behavior as a deformable solid material. The relation between the mechanical stress and the mechanical load applied to a bulk material is given by Relation (4).

$$\sigma_{ij} = \frac{F_{ij}}{S} \qquad (4)$$

Fij is the component of $\underset{e}{\rightarrow}_i$ vector-force acting on the face j (N), S is the area on which the force is acting on (m²), and σ_{ij} homogeneous components to stresses (N.m-²). In the orthonormal base $\underset{e}{\rightarrow}_1 \underset{e}{\rightarrow}_2 \underset{e}{\rightarrow}_3$, the stress state is described by Tensor (5).

$$\sigma = \begin{pmatrix} \sigma_{11} & \sigma_{12} & \sigma_{13} \\ \sigma_{21} & \sigma_{22} & \sigma_{23} \\ \sigma_{31} & \sigma_{32} & \sigma_{33} \end{pmatrix} \qquad (5)$$

In general, the diagonal terms are defined as the normal stresses and the off-diagonal terms as the shear stresses. The latter are often written τij. As a result, the stress tensor can be described by Tensor (6).

$$\sigma = \begin{pmatrix} \sigma_{11} & \tau_{12} & \tau_{13} \\ \tau_{21} & \sigma_{22} & \tau_{23} \\ \tau_{31} & \tau_{32} & \sigma_{33} \end{pmatrix} \qquad (6)$$

Normal stress can also be on tensile or compressive mode. This depends on the "+" or "-" sign of the applied loading. To study the mechanical behavior under compression of a solid material,

the classical test is made by a mechanical load of a sample surface and by the record of its length changes.
By the end of the test, the stress-strain curve is drawn. Figure 2 is an example of a stress-strain curve. Strain is the relative change in length under applied stress. Compressive stress that shortens an object gives a negative strain.
The uniaxial strain can be calculated using Eq. (7).

$$\epsilon = \frac{l - l_0}{l_0} \qquad (7)$$

Where l and l_0 are respectively the initial and the final length (or dimension) of the sample.

The curve obtained with the compression test is used to determine the elastic limit, the proportionality limit, the yield point, the yield strength, and the compressive strength as shown in Fig. 2. These parameters are used to describe the mechanical behavior of the material under compressive stress.

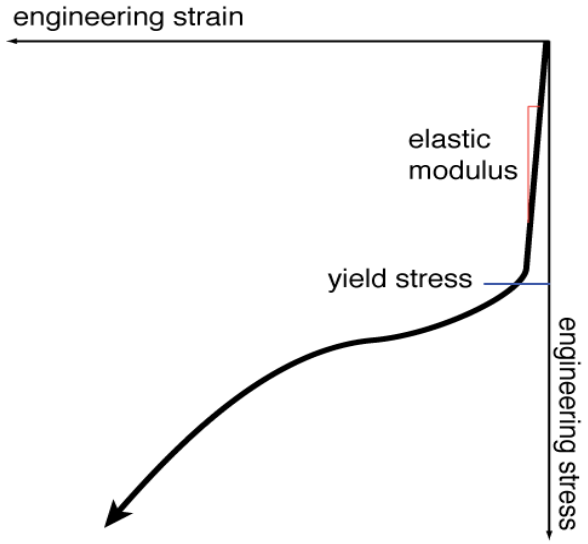

Fig. 2. Mechanical stress versus strain from a compressive test.

The curve presents two regions. The first region reveals a linear relationship between stress and strain. The slope of this curve gives the elastic (or Young's) modulus.
This relationship between stress and strain can be described by the Hooke's Law (8).

$$\sigma_{ij} = C_{ijkl}\varepsilon_{kl} \qquad (8)$$

In the second region, the stress-versus-strain relationship becomes nonlinear. Increasing the force exceeds the capacity of a material and this results in a permanent deformation. The point of transition between both behaviors is known as the compressive yield point or compressive yield stress.
The GDL does not have a clear defined mechanical behavior. Basically, this depends on the fibres distribution, the layer composition, and on the manufacturing process [33]. The compression tests applied to the GDL have shown a decrease of the electrical contact resistance under any compressive stress levels [34]. In other studies, the compression analyses of the MEA have shown that the GDLs are exposed to inhomogeneous pressures which can locally exceed

10 Mpa. Furthermore, a mechanical nonlinear behavior is observed. The addition of PTFE or MPL has a clear impact on this nonlinear behavior [28]. The loading / unloading cycles have also a strong influence on the GDL key parameters [35].

Residual deformation and layer damage

The excessive mechanical interne pressure causes a plastic deformation of the GDL, against the surface contact of the bipolar plate, and leads to a structural deformation called “tenting” (see Fig. 3 - left). At the other side of the GDL (GDL – electrode interface), the swelling of the membrane can be inhomogeneous (due to local inhomogeneous rates of humidity). This leads to a difference of mechanical pressure and may locally cause a mechanical distortion of the FC components (MEA) [30, 31].

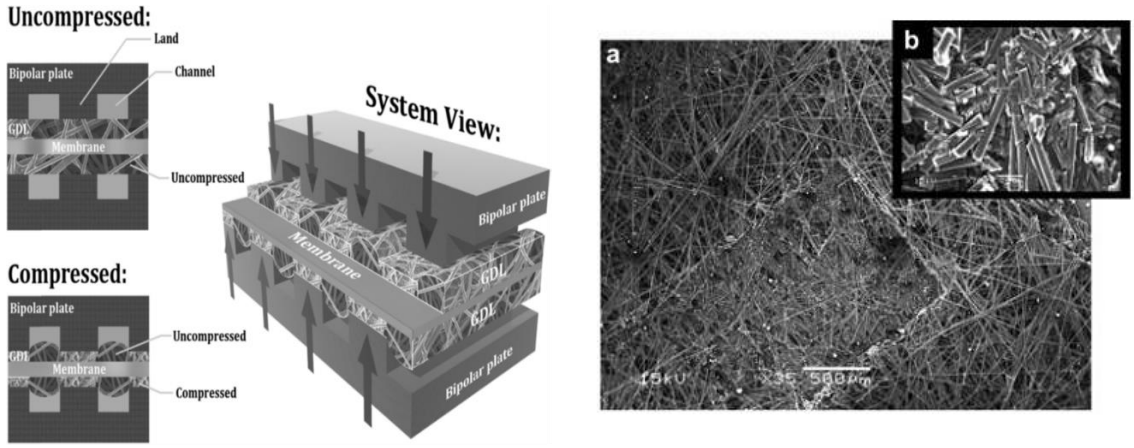

Fig. 3. Illustration of the GDL “tenting” deformation [30] (left) and effect of compression on a GDL (right).

The structural modifications, illustrated by the thickness changes, the fibres displacement and cracks over time (see Fig. 3 (right)), interact with other phenomena in the FC system. This complex problem may impact the reactants flow and the electrical transport parameters in the system. This leads finally to the decrease of the FC efficiency and to the cell degradation.

Electrical behavior and contact resistance

The capacity of a GDL to transport electrons is ensured by the carbon fibres and can be measured under three forms: in-plane, through-plane, and contact resistance.

The electrical behavior of a GDL is a function of its thickness, electron conductivity, and porosity. However, GDL presents a randomness structure. Various studies focus on the relation between this structure and a change of the GDL electrical behavior on the overall cell performance.

Zhou et al. [5] have analytically studied the effect of the electrical resistance of the GDL on its performance in a PEMFC by considering the anisotropic nature of the GDL structure. They have found that the GDL through and in-plane resistances can be neglected as they have little effect on the overall cell performance. However, the contact resistance between the PEMFC components has a significant effect, especially between the bipolar plate and the GDL.

When clamping pressure and intern compression increase, the layer thickness decreases and this phenomenon directly affects the electrical contact resistance between components.

Ahmad El-kharouf et al. [6] have studied the electrical contact resistance and the electrical in-plane resistance of a large set of commercial GDLs under two values of compression (1.5 MPa and 2.6 MPa) using a specific device. The effects of high compression loads on contact

resistances have been analyzed in [7]. It should be noted that he behavior of the electrical contact resistance vs. the mechanical stress is nonlinear. This behavior is due to the fibres reordering during compression.
In [8], Pradeep Kumar Sow et al. report a novel characterization technique and experimental setup with the aim to separately evaluate the interfacial and bulk components of the through-plane electrical resistance of a GDL. The experimental evaluation of the GDL - bipolar plate interface and GDL bulk electrical resistivity was performed as a function of clamping pressure and Teflon content for graphite and stainless steel bipolar plates, and for a GDL with and without an MPL. The measured GDL bulk resistance was found to be at most 10% of the total Ohmic resistance.

4. Experimental studies

Ex-situ characterization
The ex-situ experimental process developed is the combination of three elements: a Dynamic Mechanical Analysis (DMA) test machine, a dedicated experimental approach, and a specific method to extract the electrical contact resistance (TLM Method). A sample holder, depicted in Fig. 4, has been designed to conduct the experimental process. Then, the GDL sample can endure mechanical excitation / solicitation close to the operating conditions as cyclic mechanical compressions, mechanical static compression pre-loads, and dynamic loads, if necessary.

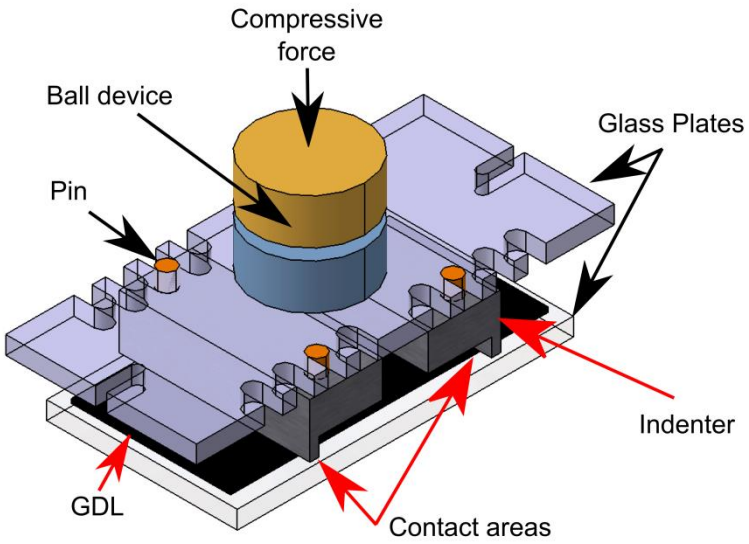

Fig. 4. Scheme of the specific sample holder used to measure the electrical contact resistance.

The measurements were performed with a Metravib VA2000 DMA machine (Fig. 5). The machine has force and displacement sensors. It also allows applying a given load in a quasi-static mode, while increasing the value of displacement in real time. The software displays the data points and the movement in real time too. This device can apply a maximal force of 64 N. With a contact surface of 3 mm² (contact areas of the indenters in Fig. 5), a stress value of 10.67 MPa can be achieved.
In order to study the electrical behavior under a given stress, the sample holder is electrically connected to a voltage generator (Tektronix TDS 2002). Current and voltage between the measurements points are recorded with a specific acquisition card.

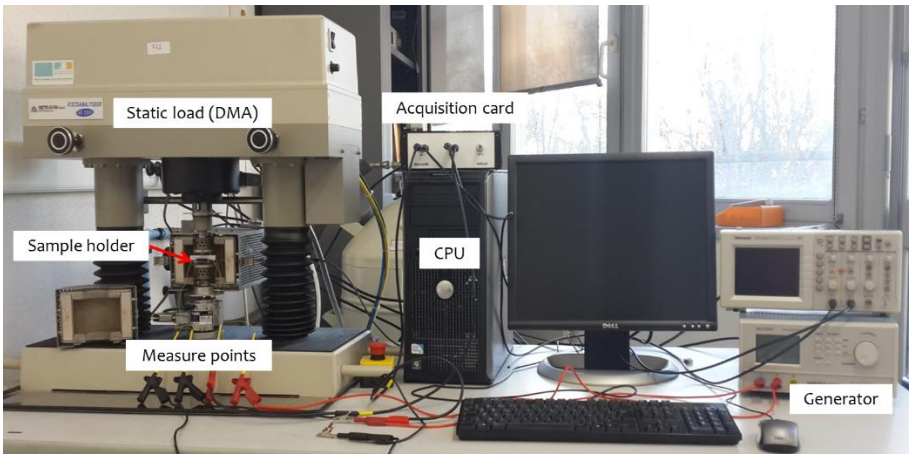

Fig. 5. Test bench for GDL ex-situ characterization.

Objective (operating conditions)

To understand the GDL behavior inside the stack, we should duplicate the PEMFC operating conditions, in terms of compression, cell potential, temperature and humidity.

As already mentioned, the first studies made in this work were focused on the electrical / mechanical coupling. During the tests, we applied a load to achieve some stress levels ranging from 0.4 MPa to 10.67Mpa. The applied voltage on the GDL terminals was fixed at 0.6 V. The test was performed at ambient room temperature and humidity.

Principle of resistance measure with Transfer Length Method (TLM)

The TLM method is a specific method to characterize the electrical contact resistance between metal and semiconductor. This method was proposed by W. Shockley in 1964 [36]. We present below some information regarding the mathematical model associated to TLM, as well as the characteristics of the materials involved in the tests.

This technique is based on the measurement of the total electric resistance (Rt) between two metal terminals by measuring current (I) – voltage (V) curves. The electrical contact resistance (Rc) and the electrical in-plane resistance (Rs0) are calculated from the Rt curve as a function of the spacing (d) between both indenters of the set-up in Fig. 4.

Applying a voltage between the two contacts / indenters and measuring the electric current allows computing the resistance between these two contacts. This is true under the following assumptions:

- the massive resistance of the indenter is negligible (the value is very low since it is supposed to be a massive metal),
- the resistance of the compressed GDL related to RS_0 is neglected. This is verified by the linearity of the (R_t=f(d)) curve obtained (there is no edge effect).

As shown in Fig. 6, this resistance can be considered as the sum of the resistances of the two contacts (assumed equal and denoted Rc) and the resistance of the GDL between the two contacts (noted Rs_0).

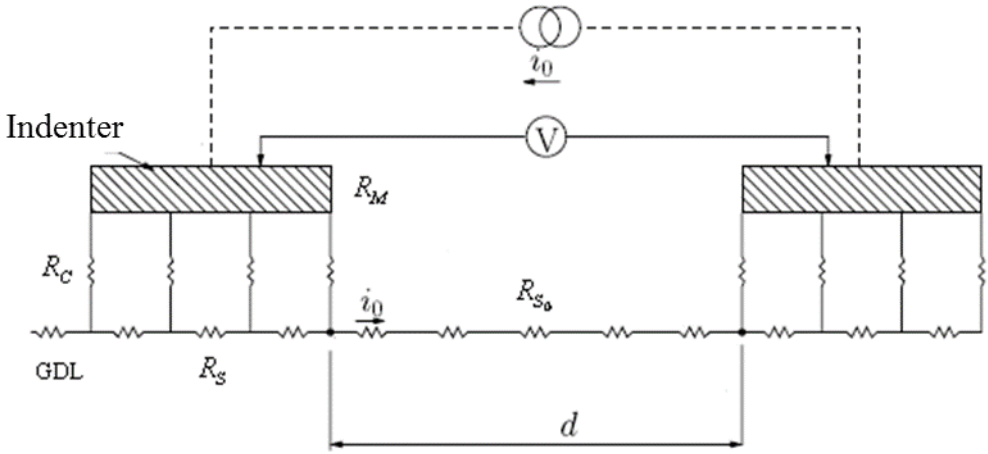

Fig. 6. Description of the different resistances involved in the TLM method.

R_{S0} (Ω.cm²): Resistance of GDL out of contact.
R_S: Resistance of GDL under contact.
R_M: Resistance of coated steel (indenter).
R_T: Total resistance.
R_c: Contact resistance.
d: Distance between indenters.

On the basis of the TLM mathematical model shown in Fig. 6, the total electric resistance (Rt) can be computed using Eq. (9) and (10).

$$R_t(d) = 2R_c + R_{s0}(d) \qquad (9)$$

With:

$$R_{s0}(d) = \frac{d}{W} R_{s0} \qquad (10)$$

Once the resistance Rt(d) is measured between two consecutive contacts (Fig. 7), we can draw the curve of resistors Rt versus d (Fig. 8).

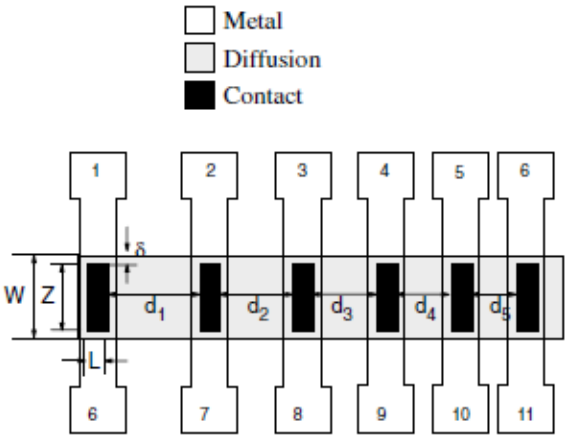

Fig. 7. Description of the measurement by the TLM method.

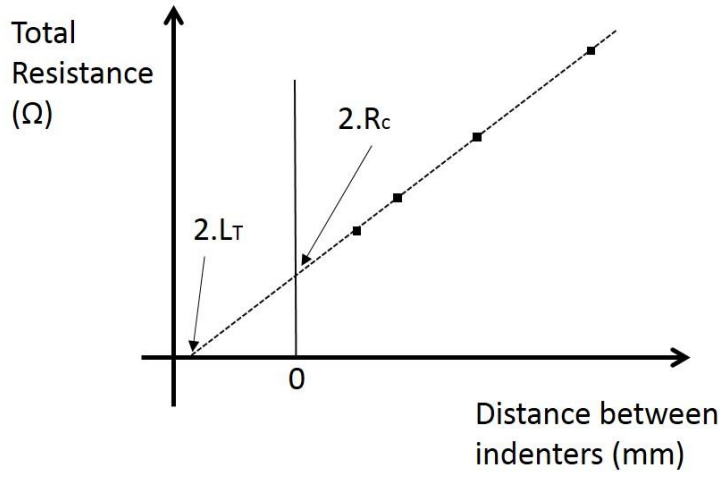

Fig. 8. Total resistance versus distance between the two indenters.

In Fig. 8, the point of interception between the curve and the vertical axis gives access to the electrical contact resistance Rc. The slope, according to Eq. (9), is dRS_0 / W, which allows evaluating the resistance square of the layer, and thus its in-plane resistivity in the case of a homogeneous materials and a known thickness.

We can find two types of contact: vertical contact and horizontal contact. In the case of vertical contacts (flow lines are perpendicular to the interface), the resistance of a contact is inversely proportional to its area. In the second case, the current density through the GDL varies from one point to another point of the contact interface. This is due to the concentration phenomenon of current lines at the contact areas.
The tendency of a horizontal contact to spread the current lines is characterized by its transfer length L_T. A high transfer length means that the contact will have a sufficient length which will not limit the current flow. This parameter is important in order to predict the minimum length of the contact. This is necessary to remove the effect of resistance R_C. In practice, it is considered that 3-5 L_T is sufficient for the length of the contact. The L_T parameter is a function of the deposited metallization (resistivity $\rho_c$and resistance), and the GDL resistance through the contact (see Eq. 11).

$$L_t = \sqrt{\frac{\rho_c}{R_s+R_M}} \qquad (11)$$

Electrical circuit
The study first aims at determining the total strength of the material from a current imposed by a specific electrical circuit. The drive voltage is applied with the Tektronix TDS 2002 generator (Fig. 5). As mentioned before, the measured current is the one that crosses the resistance of 20 Ohms and is recorded as a voltage thanks to the acquisition card. The precision of this map is 2 mV; the measured current has an accuracy of 0.1 mA.

Originality of the testing apparatus
The test bench has already been used for the analysis of thermomechanical behaviors of various organic materials and composites. It was also used to achieve creep and relaxation tests. We have exploited its capabilities through the use of an in-house sample holder designed to be both adapted for the DMA machine and the ex-situ measurements of different GDL properties.

First, to have representative results for the FC stack, the indenter is designed to have a representative dimension of flow field contacts. A gold layer was deposited to minimize the electric resistance of the indenters and to produce a reference result.
The second point is the mechanical consistency of the results. The mechanical loading must be distributed in a uniform way across the surface of GDL. This is an essential condition to ensure the relevance of the results.
The sample holder is specifically designed in a way to guarantee the uniform load for the whole measurement surface. A ball device is used for this function. The electrical insulation is guaranteed by glass plates.

5. Results and discussion

The objective of this study is to obtain a better understanding of the GDL – plate set electrical behavior under stress. The stress-strain curves are plotted from experimental test results. The compression-creep tests are carried out on different GDL references (Table 1).

Table 1. GDL technical specifications (SGL Carbon company).

GDL reference	Thickness Sample (µm)	PTFE addition (wt %)	MPL addition
SGL 24 AA	190±30	0	No
SGL 24 BA	190±30	5	No
SGL 24 BC	235±30	5	Yes

The GDLs are made of carbon fiber, and some of them are loaded with PTFE or coated with a microporous sublayer (MPL). The GDL 24 BC undergoes a treatment with PTFE and has a MPL.
We consider the behavior of the GDL under static load. An illustration is given in Fig. 9 to show the temporal variation shapes of the applied mechanical force.
The experimental results are stored as an array of points in a text file and the whole information is then treated under the Matlab software environment. Then strain and stress are calculated using Eq. (4) and (6).

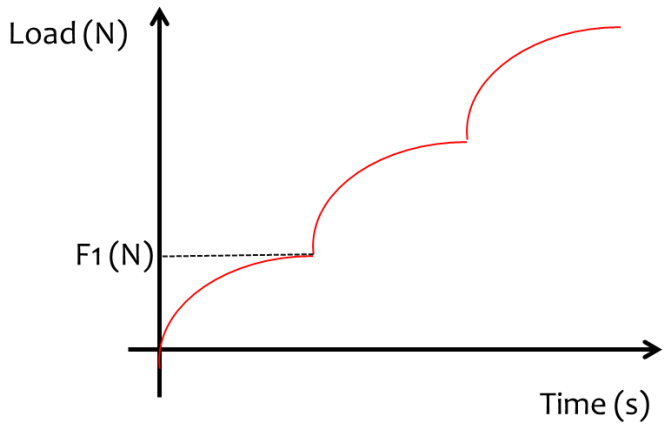

Fig. 9. Illustration of the force applied during the test.

To increase the maximum compressive stress that can be applied to a sample, the GDL samples are cut in smaller parallelepiped with a width of 3 mm. As already mentioned, this results in a maximum compression pressure of 10.67 MPa. The intern compressive stress in a PEFC can

reach 10 MPa [28]. Therefore, the purpose of the study is to extend the range of the stress test. In order to stabilize the mechanical behavior of the GDL, 5 loading / unloading cycles varying between 0 and Fmax equal to 65 N are applied to the GDL [35].

5.1. Study of the measurement stability and repeatability

Before initiating the test, as already mentioned, the aim is to approach as closely as possible with our set-up the reality of the physical phenomena inside the stack. Table 2 shows the test conditions.

Table 2. Experimental parameters and conditions selected for the tests.

Load levels	Distance (mm)	Voltage (V)	Repeatability of test
10, 20, 30, 40, 50, and 60 N Test with SGL 24AA SGL 24BA SGL 24BC	1,5	6	The tests are made 3 times after 7 cycles of loading – unloading.
	9,28	6	
	18	6	
	26	6	

To choose these parameter values, some preliminary studies were performed in order to observe the effect of the chosen levels on the measurements. The first parameter investigated was the voltage imposed by the power generator (Fig. 5).

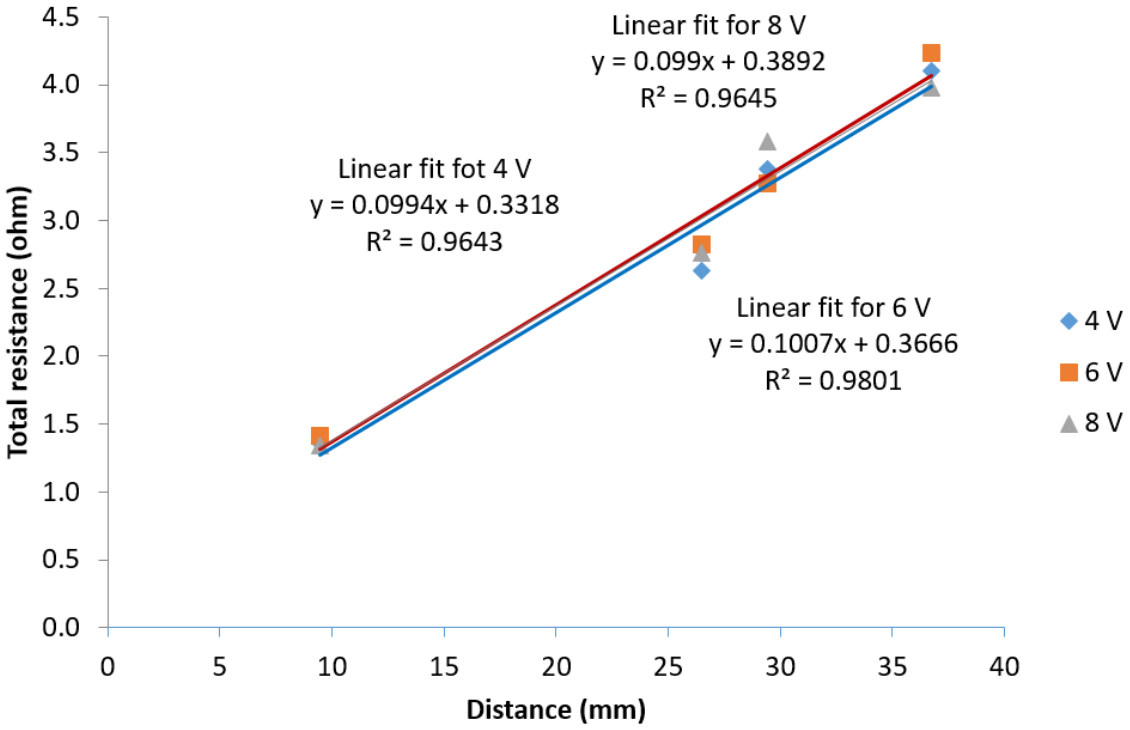

Fig. 10. Total resistance versus distance between indenters for three different voltages imposed with the electrical generator.

We applied three different potential values (4V, 6V, and 8V) in order to evaluate the effect of the voltage value applied at the GDL terminals on the resistance measurement under the loading. Figure 10 shows that the change of the applied voltage has a negligible effect on the measured contact resistance.

5.2 Effect of PTFE on GDL stress strain curve

To ensure the gas flow through the GDL and the water management, the fibers are treated with a hydrophobic agent (PTFE). It leads to a structural effect and arrangement of the fibers, but it induces also some changes of the physical properties. Many research works were conducted on PTFE effect over the gas diffusion properties as the permeability [37], whereas the effect of this additive on the mechanical behavior has been less studied [16].
Figure 11 presents the stress-strain curves of the three GDLs SGL 24AA, SGL 24BA and SGL 24BC with different PTFE contents. One can notice that the three curves show similar shapes, as the base material is the same (carbon fiber). The loading with PTFE effect becomes more significant after a stress of 2 MPa. In this first part, the GDL thickness continues to decrease due to the rearrangement of the fibers and their compaction. Beyond this stress value, the GDL with SGL 24BC and SGL 24BA references have higher compressive resistances than the untreated GDL SGL 24 AA. This is due to the presence of PTFE that coats the fibers for granted over compressibility resistance.
The presence of MPL that contains a significant proportion of PTFE increases the resistance, which is illustrated in Fig. 11 by the difference between the GDL SGL 24 BC and the GDL SGL 24 BA.

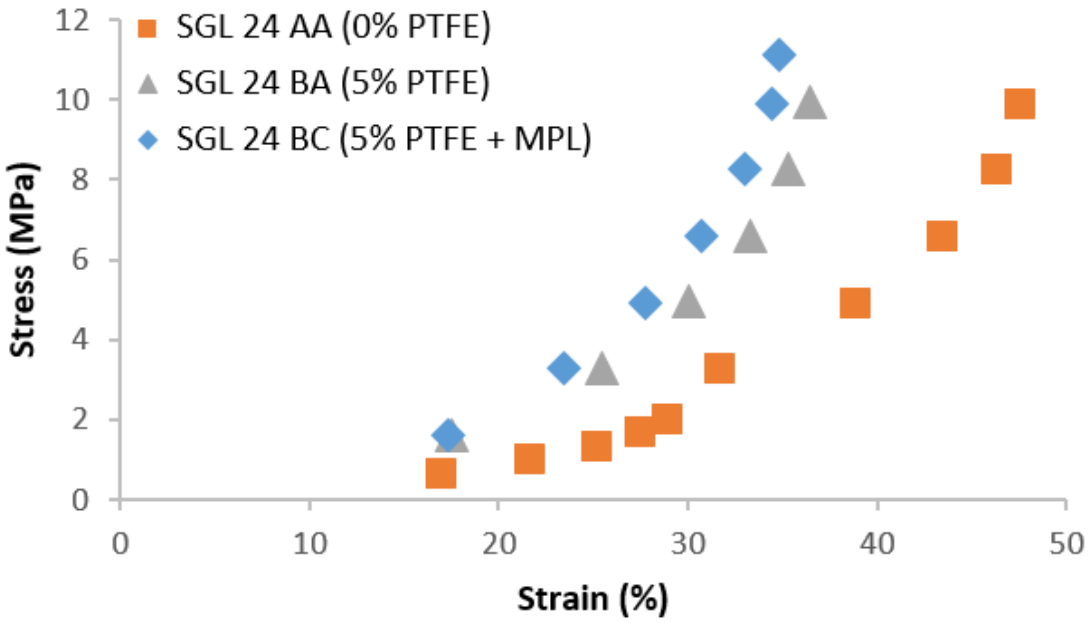

Fig. 11. Stress-strain curves for three GDLs.

For the highest constraints applied on a GDL, we can observe a kind of trend curve showing a limit value of deformation. This is due that the GDL is fully compressed. Beyond this stage, we could cause any damages in the layers and any fiber cracks.

5.3. Effect of compression on contact resistance curve

A commercial GDL was selected and studied. First, the GDL achieved seven compressive cycles from 0 to 60 N before the measurements, in order to stabilize the mechanical behavior. The measurements were made at different static compressive (homogenous compression) loads at room temperature, with our set-up described above, and using a GDL sample with a 3x2 mm2 affected area. The relationship between the contact resistance and the mechanical compressive load is shown in Fig. 12.

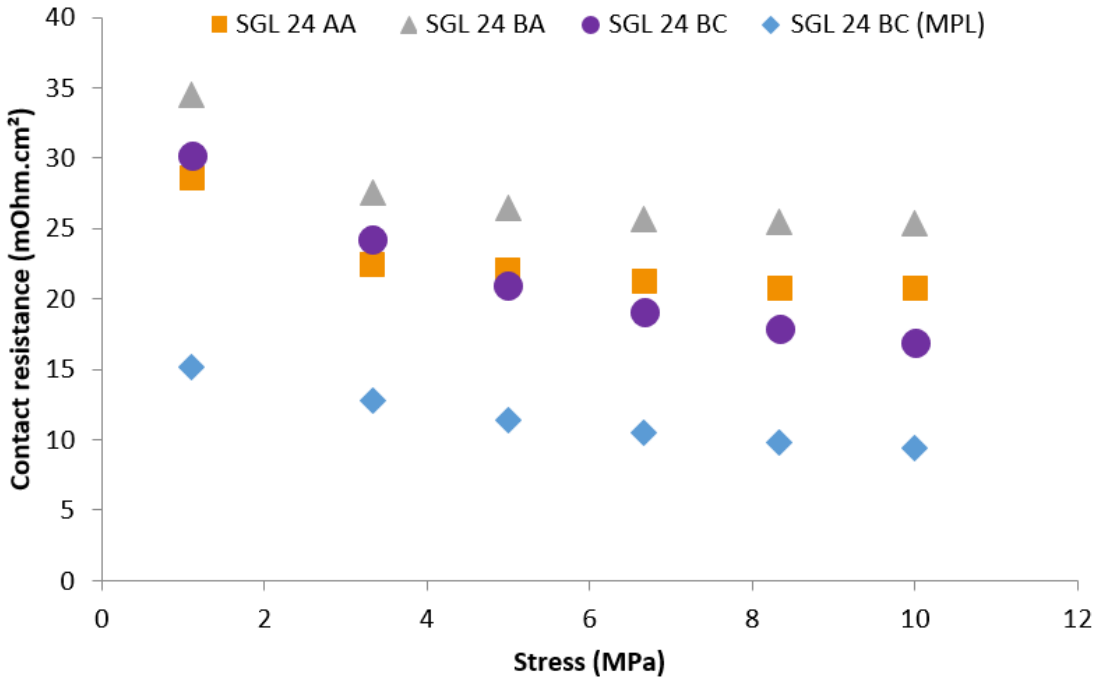

Fig. 12. Electrical contact resistance versus mechanical static compression stress (GDLs ref. SGL 24 AA, SGL 24 BA and SGL 24 BC).

A nonlinear decrease of the contact resistance with stress can be observed. Under high mechanical stress, the resistance tends towards a constant value. An exponential function can fit the experimental curve of the contact resistance. The contact resistance decreases dramatically from 38 mohm.cm^2 to 22 mohm.cm^2 under 3 MPa stress. This result gives an idea on how the increased internal pressure may drive a change of the electric behavior in the stack. The behavior observed is due to the improvement of the contact between the indenters and the GDL during the compression phase. This process suggests that a higher fiber density facilitates the transfer of a larger electron flow. Secondly, compressing the GDL leads to a structural modification, which causes a decrease of the porosity. This loss affects other properties like permeability, thermal conductivity, and water management.
According to the last results, we can establish a relationship between the compression capacity of the GDL (stress-strain curves) and the change of the contact resistance.

The GDL SGL 24 BC presents a low contact resistance, in particular for the MPL side, as long as stress strain curve has a significant deformation of 48%. As a result, an irreversible mechanical behavior is able to induce any damage to the layer after a number of loading-unloading cycles under operating conditions.

The presence of PTFE leads to an improvement of the resistance to deformation under increased pressure. But instead both SGL 24 BA and 24 BC present larger contact resistances than SGL 24 AA.
GDL ref. SGL 24 BC (MPL) is coated with a microporous layer. To highlight the effect of this layer on the contact resistance, we chose to achieve some tests on the MPL-side. Figure 12 shows that the contact resistance between the MPL and the indenter is smaller than the resistance between the GDL and the indenter.

6. Conclusion

As PEMFC technology becomes gradually mature for a widespread marketing, so the research and innovation conducted in the mechanical field grow in importance. To reach the various requirements in terms of durability and reliability, the mechanical constraints must be taken into account during the design process of FC stacks and the selection of the well-suited components.

The work described in this article focus on the electrical – mechanical behavior of GDLs for PEMFC stacks. The GDL mechanical / materials properties play a key-role in the achievement of high cell performances. In particular, the GDL is the component that is subject to the strongest deformation. Especially the contact resistance between the GDL and the flow field plate needs to be studied. It has to be determined by considering different mechanical loads related both with the internal cell pressure due to the thermal expansion of the MEA components and the external clamping pressure applied to the cell or stack assembly.

In this paper, we have described an experimental set-up (and the related protocols) that can be used as an ex-situ tool to determine the contact resistances of different GDL references (and materials). The electrical measurements are done while imposing mechanical loads to the tested GDLs. Particular attention was paid to the definition of a preconditioning procedure made of different loading / unloading cycles in order to stabilize the mechanical behavior of the GDLs and increase the relevancy of the results.

A nonlinear behavior of the electrical contact resistance versus the mechanical stress was observed in the experiments. After applying a mechanical pressure of 5 MPa, some constant values were obtained for the three commercial GDLs. This behavior is due to the GDL fibres reordering during compression up to the reaching of the physical compaction limit. During testing, we could also identify the effect of the GDL composition on the mechanical and electrical test responses. The impact of the PTFE on the GDL behavior was observed. The increase of the compression resistance was linked to the presence of this additive. This change in the compression behavior leads to an increase of the electrical resistance.
Through the experiments, we could develop a better understanding of the relationship between the GDL mechanical behavior and its electrical contact resistances. The set-up will allow building a database of GDL electrical – mechanical characteristics, which can be useful to obtain a better understanding of GDL behaviors, to feed with GDL data some more global multi-physical FC models, to help FC manufacturers in the stack design and in the selection of suitable components.

Further works will deal with the investigation of mechanical – electrical GDL properties under real FC operating conditions including thermal and humidity variations.

Acknowledgments
The “Région Franche-Comté” is gratefully acknowledged for its support through the funding of Soufiane El Oualid Master’s thesis in the frame of the project ELICOP (Ref. 2015C-4944 and 2015C-4948).

7. References

[1] A Alaswad, A Baroutaji, H Achour, J Carton, Ahmed Al Makky, AG Olabi. Developments in fuel cell technologies in the transport sector. International Journal of Hydrogen Energy 2016; 41(37):16499-16508.

[2] Tabbi Wilberforce, A Alaswad, A Palumbo, M Dassisti, AG Olabi. Advances in stationary and portable fuel cell applications. International Journal of Hydrogen Energy 2016; 41(37):16509-16522.

[3] C-C Chen, D Shaw, K-L Hsueh. Optimization of the electrodes humidification temperature and clamping pressure to achieve uniform current density in a commercial-sized proton exchange membrane fuel cell. International Journal of Hydrogen Energy, In Press, Corrected Proof, Available online 14 October 2016.

[4] D Singdeo, T Dey, PC Ghosh. Contact resistance between bipolar plate and gas diffusion layer in high temperature polymer electrolyte fuel cells. International Journal of Hydrogen Energy 2014; 39(2):987-995.

[5] P Zhou, CW Wu, GJ Ma. Contact resistance prediction and structure optimization of bipolar plates. Journal of Power Sources 2006; 159(2):1115-1122.

[6] Ahmad El-kharouf, Thomas J Mason, Dan JL Brett, Bruno G Pollet. Ex-situ characterisation of gas diffusion layers for proton exchange membrane fuel cells. Journal of Power Sources 2012; 218:393-404.

[7] R Montanini, G Squadrito, G Giacoppo. Measurement of the clamping pressure distribution in polymer electrolyte fuel cells using piezoresistive sensor arrays and digital image correlation techniques. J Power Sources 2011;196(20):8484-8493.

[8] PK Sow, S Prass, P Kalisvaart, W Mérida. Deconvolution of electrical contact and bulk resistance of gas diffusion layers for fuel cell applications. International Journal of Hydrogen Energy 2015; 40(6):2850-2861.

[9] S Tanaka, T Shudo. Experimental and numerical modeling study of the electrical resistance of gas diffusion layer-less polymer electrolyte membrane fuel cells. Journal of Power Sources 2015; 278:382-395.

[10] J Millichamp, TJ Mason, TP Neville, N Rajalakshmi, R Jervis, PR Shearing, DJL Brett. Mechanisms and effects of mechanical compression and dimensional change in polymer electrolyte fuel cells – A review. Journal of Power Sources 2015; 284:305-320.

[11] M Hamour, JC Grandidier, A Ouibrahim, S Martemianov. Electrical conductivity of PEMFC under loading. Journal of Power Sources 2015; 289:160-167.

[12] Devin Todd, Scott Bennett, Walter Mérida. Anisotropic electrical resistance of proton exchange membrane fuel cell transport layers as a function of cyclic strain. International Journal of Hydrogen Energy 2016; 41(14):6029-6035.

[13] DM Fadzillah, MI Rosli, MZM Talib, SK Kamarudin, WRW Daud. Review on microstructure modelling of a gas diffusion layer for proton exchange membrane fuel cells. Renewable and Sustainable Energy Reviews, In Press, Corrected Proof, Available online 5 December 2016.

[14] S Tanaka, WW Bradfield, C Legrand, AG Malan. Numerical and experimental study of the effects of the electrical resistance and diffusivity under clamping pressure on the performance of a metallic gas-diffusion layer in polymer electrolyte fuel cells. Journal of Power Sources 2016; 330:273-284.

[15] C Carral, N Charvin, H Trouvé, P Mélé. An experimental analysis of PEMFC stack assembly using strain gage sensors. International Journal of Hydrogen Energy 2014; 39(9):4493-4501.

[16] Sogol Roohparvarzadeh. Experimental Characterization of the Compressive Behaviour of Gas Diffusion Layers in PEM Fuel Cells. Thesis, Master of Applied Science in Mechanical Engineering, University of Waterloo, Ontario, Canada, 2014. 89 Pages.

[17] OM Orogbemi, DB Ingham, MS Ismail, KJ Hughes, L Ma, M Pourkashanian. The effects of the composition of microporous layers on the permeability of gas diffusion layers used in polymer electrolyte fuel cells. International Journal of Hydrogen Energy 2016; 41(46):21345-21351.

[18] M Fazeli, J Hinebaugh, Z Fishman, C Tötzke, W Lehnert, I Manke, A Bazylak. Pore network modeling to explore the effects of compression on multiphase transport in polymer electrolyte membrane fuel cell gas diffusion layers. Journal of Power Sources 2016; 335:162-171.

[19] IV Zenyuk, DY Parkinson, LG Connolly, AZ Weber. Gas-diffusion-layer structural properties under compression via X-ray tomography. Journal of Power Sources 2016; 328:364-376.

[20] F Lapicque, M Belhadj, C Bonnet, J Pauchet, Y Thomas. A critical review on gas diffusion micro and macroporous layers degradations for improved membrane fuel cell durability. Journal of Power Sources 2016; 336:40-53.

[21] Xiao-Zi Yuan, Haijiang Wang. PEM Fuel Cell Fundamentals. In: PEM Fuel Cell Electrocatalysts and Catalyst Layers: Fundamentals and Applications. Edited by Jiujun Zhang. Springer-Verlag London, 2008. Pages 1-79. ISBN: 978-1-84800-935-6 (Print) 978-1-84800-936-3 (Online). DOI 10.1007/978-1-84800-936-3.

[22] Rama P, Chen R, Andrews JD. A review of performance degradation and failure modes for hydrogen-fuelled polymer electrolyte fuel cells. Proceedings of the Institution of Mechanical Engineers, Part A: Journal of Power and Energy 2008; 222(5):421-441. [DOI: 10.1243/09576509JPE603].

[23] R. Taspinar, S. Litster, E.C. Kumbur. A computational study to investigate the effects of the bipolar plate and gas diffusion layer interface in polymer electrolyte fuel cells. International Journal of Hydrogen Energy 2015; 40(22):7124-7134.

[24] Prafful Mangal, Lalit M. Pant, Nicholas Carrigy, Mark Dumontier, Valentin Zingan, Sushanta Mitra, Marc Secanell. Experimental study of mass transport in PEMFCs: Through plane permeability and molecular diffusivity in GDLs. Electrochimica Acta 2015; 167:160-171.

[25] Yu M Volfkovich, VS Bagotzky. The method of standard porosimetry: 1. Principles and possibilities. Journal of Power Sources 1994; 48(3):327-338.

[26] Yu M Volfkovich, VS Bagotzky. The method of standard porosimetry 2. Investigation of the formation of porous structures. Journal of Power Sources 1994; 48(3):339-348.

[27] Yu-Xian Huang, Chin-Hsiang Cheng, Xiao-Dong Wang, Jiin-Yuh Jang. Effects of porosity gradient in gas diffusion layers on performance of proton exchange membrane fuel cells. Energy 2010; 35(12):4786-4794.

[28] Y Faydi, R Lachat, P Lesage, Y Meyer. Experimental Characterization Method of the Gas Diffusion Layers Compression Modulus for High Compressive Loads and Based on a Dynamic Mechanical Analysis. Journal of Fuel Cell Science and Technology 2015; 12(5). 5 pages.

[29] Y Faydi, R Lachat, Y Meyer. Thermomechanical characterisation of commercial Gas Diffusion Layers of a Proton Exchange Membrane Fuel Cell for high compressive pre-loads under dynamic excitation. Fuel 2016; 182:124-130.

[30] Thomas J Mason, Jason Millichamp, Paul R Shearing, Daniel JL Brett. A Study of the Effect of Compression on the Performance of Polymer Electrolyte Fuel Cells Using Electrochemical Impedance Spectroscopy and Dimensional Change Analysis. International Journal of Hydrogen Energy 2013; 38(18):7414-7422.

[31] Thomas J Mason, Jason Millichamp, Tobias P Neville, Paul R Shearing, Stefaan Simons, Daniel JL Brett. A study of the effect of water management and electrode flooding on the dimensional change of polymer electrolyte fuel cells. Journal of Power Sources 2013; 242:70-77.

[32] J Zachary Fishman, Hilary Leung, A Bazylak. Droplet pinning by PEM fuel cell GDL surfaces. International Journal of Hydrogen Energy 2010; 35(17):9144-9150.

[33] Ahmaf El-Kharouf. Understanding GDL properties and performance in polymer electrolyte fuel cells. PhD Thesis. University of Birmingham, 10th March 2014.

[34] Ö Aydin, M Zedda, N Zamel. Challenges Associated with Measuring the Intrinsic Electrical Conductivity of Carbon Paper Diffusion Media. Fuel Cells 2015; 15(3):537-544.

[35] PA Gigos, Y Faydi, Y Meyer. Mechanical characterization and analytical modeling of gas diffusion layers under cyclic compression. International Journal of Hydrogen Energy 2015; 40(17):5958-5965.

[36] W Shockley. Research and investigation of inverse epitaxial UHF power transistors. Air Force Atomic Laboratory, Wright-Patterson Air Force Base, USA A1-TOR-64-20, 1964.

[37] Aydin Nabovati, James Hinebaugh, Aimy Bazylak, Cristina H Amon. Effect of porosity heterogeneity on the permeability and tortuosity of gas diffusion layers in polymer electrolyte membrane fuel cells. Journal of Power Sources 2014; 248:83-90.

Figure Captions

Fig. 1. Classical architecture of a PEMFC [16].

Fig. 2. Mechanical stress versus strain from a compressive test.

Fig. 3. Illustration of the GDL "tenting" deformation [30] (left) and effect of compression on a GDL (right).

Fig. 4. Scheme of the specific sample holder used to measure the electrical contact resistance.

Fig. 5. Test bench for GDL ex-situ characterization.

Fig. 6. Description of the different resistances involved in the TLM method.
R_{S0} (Ω.cm²): Resistance of GDL out of contact.
R_S: Resistance of GDL under contact.
R_M: Resistance of coated steel (indenter).
R_T: Total resistance.
R_c: Contact resistance.
d: Distance between indenters.

Fig. 7. Description of the measurement by the TLM method.

Fig. 8. Total resistance versus distance between the two indenters.

Fig. 9. Illustration of the force applied during the test.

Fig. 10. Total resistance versus distance between indenters for three different voltages imposed with the electrical generator.

Fig. 11. Stress-strain curves for three GDLs.

Fig. 12. Electrical contact resistance versus mechanical static compression stress (GDLs ref. SGL 24 AA, SGL 24 BA and SGL 24 BC).

Table Captions

Table 1. GDL technical specifications (SGL Carbon company).

Table 2. Experimental parameters and conditions selected for the tests.